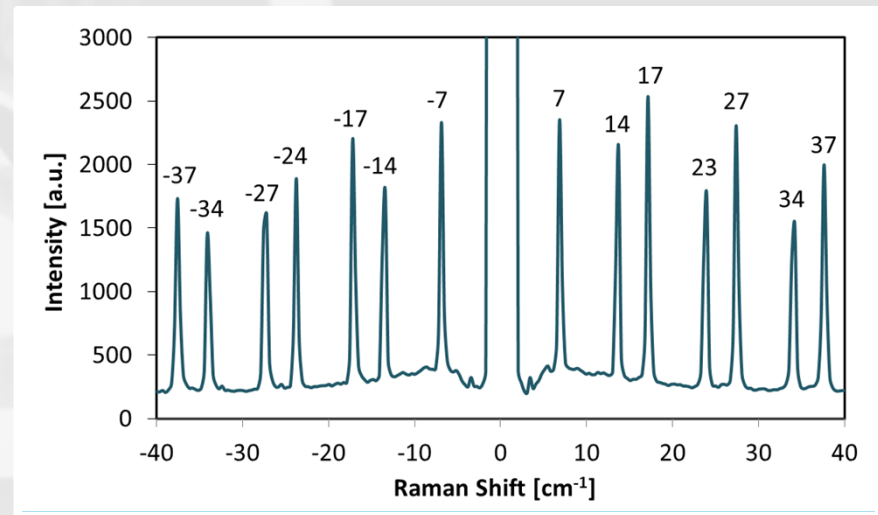
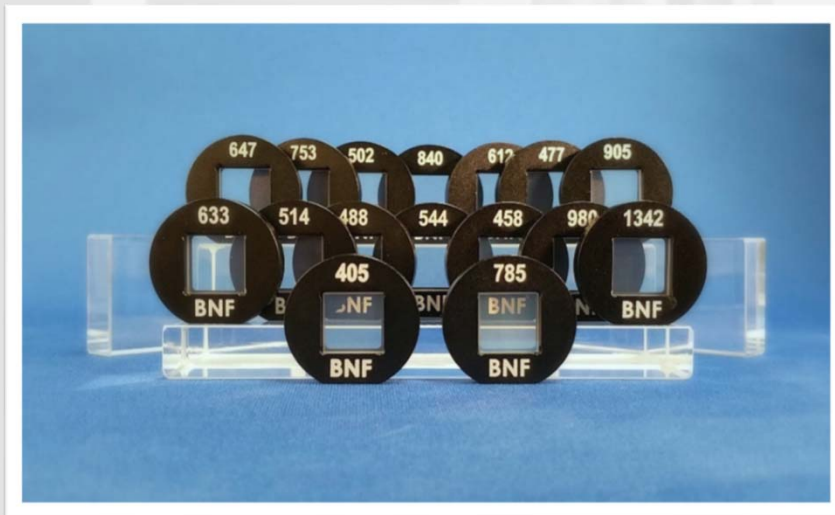


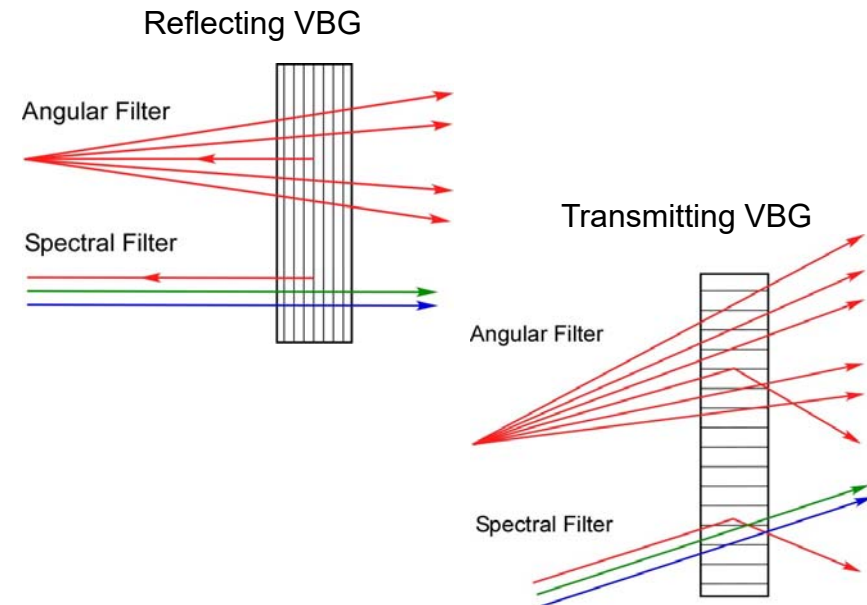
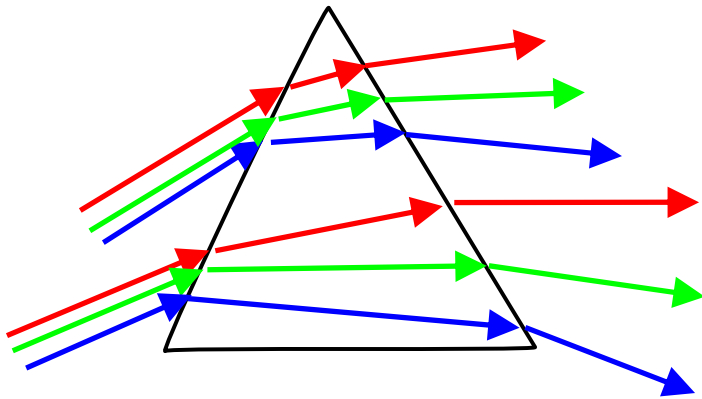
# BragGrate™ Raman Filters

## Volume Bragg Gratings for Ultra-low Frequency Raman Spectroscopy



# What is Volume Bragg Grating (VBG)?

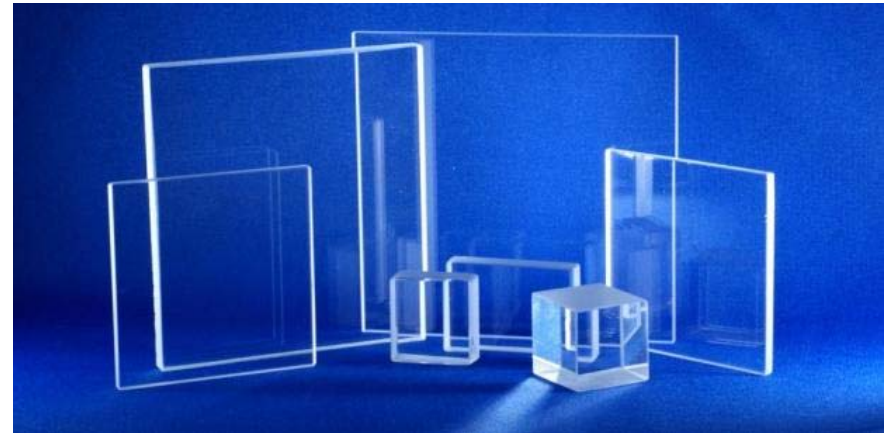
- ❖ **VBG** is a volume hologram formed by photo-induced modulation of the refractive index (RI) of the recording media
- ❖ **Volume hologram** – thickness is much larger than light wavelength
  - Diffraction is possible only at Bragg conditions => the light has to have the right wavelength and angle



- ❖ Prisms and surface gratings are conventional dispersive elements for different angles and wavelengths
- ❖ Spectral resolving power is up to 8,000
- ❖ VBG is a dispersive element for single wavelength and single angle
- ❖ Spectral resolving power up to 20,000

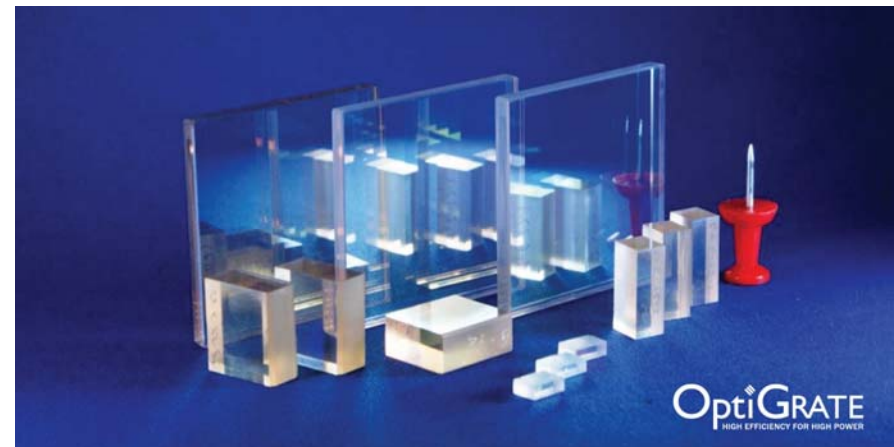
## ❖ PTR Glass

Photo-thermo-refractive glass is a sodium-zinc-aluminum-silicate glass doped with silver, cerium, and fluorine which provides RI modulation after exposure to UV radiation followed by thermal development



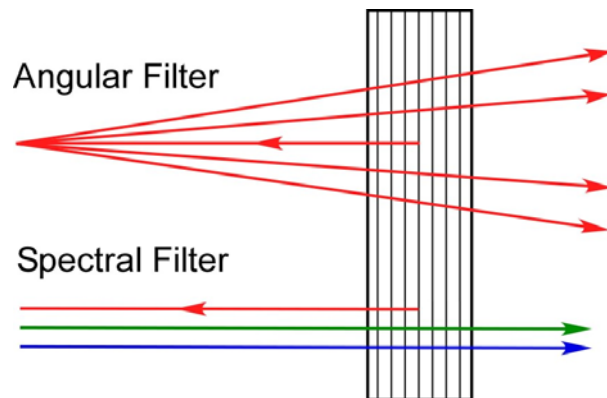
## ❖ Volume Bragg Gratings

- Reflecting Bragg Grating
- Transmitting Bragg Grating
- Multiplexed Bragg Grating
- Transverse Chirped Grating
- Chirped Bragg Grating

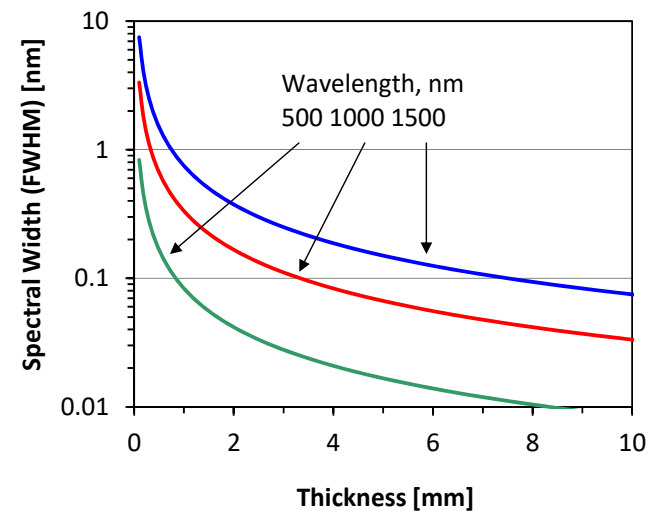


- ❖ Low-frequency Raman is an indispensable analytical tool in multiple areas of scientific research
  - Low-frequency Raman bands (lower than  $50 \text{ cm}^{-1}$ ) exist in certain proteins. They are dependent upon the conformation of the protein molecule, but are relatively independent of the form of the sample, i.e., whether it is a film or a crystal.
  - In amorphous glasses, most of the Raman spectra present a low frequency response called "boson peak".
  - Much minerals present low frequency vibration modes, i.e. sulfur between  $0$  and  $250 \text{ cm}^{-1}$ , or organic materials like L-Cystine between  $0$  and  $800 \text{ cm}^{-1}$ .
  - Single-wall and multi-wall carbon nanotubes exhibit radial breathing mode (RBM) vibrations in the range  $150$ – $200 \text{ cm}^{-1}$  which are used to characterize diameter distribution and overall quality of nanotubes as well as influence of external factors.
  - Quality of semiconductor multi-layered structures (superlattices) is assessed by observing folded acoustic (FA) modes in the range  $0$ – $100 \text{ cm}^{-1}$ .
  - The Relaxation modes in liquids, binary mixtures and solutions, in the range  $0$ – $400 \text{ cm}^{-1}$ , help to determine their dynamic structure.
  
- ❖ Selected applications of ULF Raman spectroscopy
  - Pharmaceutical polymorphs
  - LA modes of polymer
  - Semiconductor lattices and nanostructures
  - Material : phase/structure
  - Metal Halides
  - Gases
  - Carbon nanotubes
  - Micro, nano-crystallites

## Reflecting Volume Bragg Grating (RBG)



## Spectral width of RBG



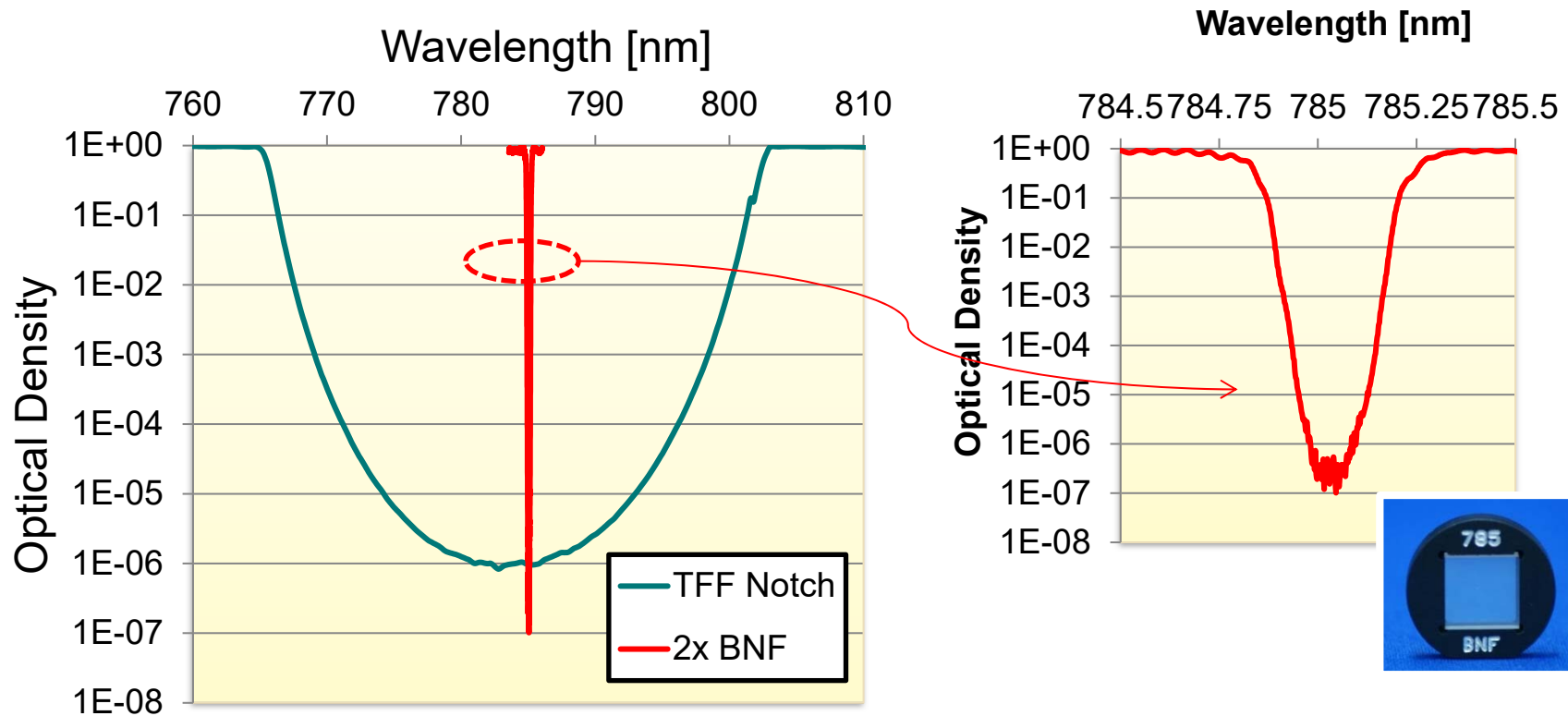
## Reflecting Volume Bragg Gratings as Raman Notch Filters

- ❖ Diffraction Efficiency (DE) up to 99.99% (standard optical density: OD>3 and OD>4)
- ❖ Spectral Bandwidth (FWHM) < 5 cm<sup>-1</sup>
- ❖ Angular Selectivity (FWHM) < 5 mrad
- ❖ Wavelength Range 400 nm to 2 μm (standard: **488, 514, 532, 633, 785, 1064 nm**) (extended: **405, 442, 458, 473, 491, 552, 561, 568, 588, 594, 660 nm**) others can be fabricated
- ❖ Grating Thickness: 2-3 mm
- ❖ Standard BNF dimensions: 11 × 11 and 12.5 × 12.5 mm<sup>2</sup> (up to 25 × 25 mm<sup>2</sup>)
- ❖ No time degradation: stable up to 400C and any type of optical and ionizing radiation

## ADVANTAGES of BragGrate™ Raman Filters

- ❖ Ultra-low frequency measurement down to 5 cm<sup>-1</sup> with single stage spectrometers
- ❖ Simultaneous measurements of both Stokes and anti-Stokes Raman bands
- ❖ No polarization dependence
- ❖ Environmentally stable, no humidity degradation
- ❖ No degradation up to 400°C
- ❖ Stable to any type of optical and ionizing radiation

# Linewidth of BragGrate™ notch filter vs thin film notch filter

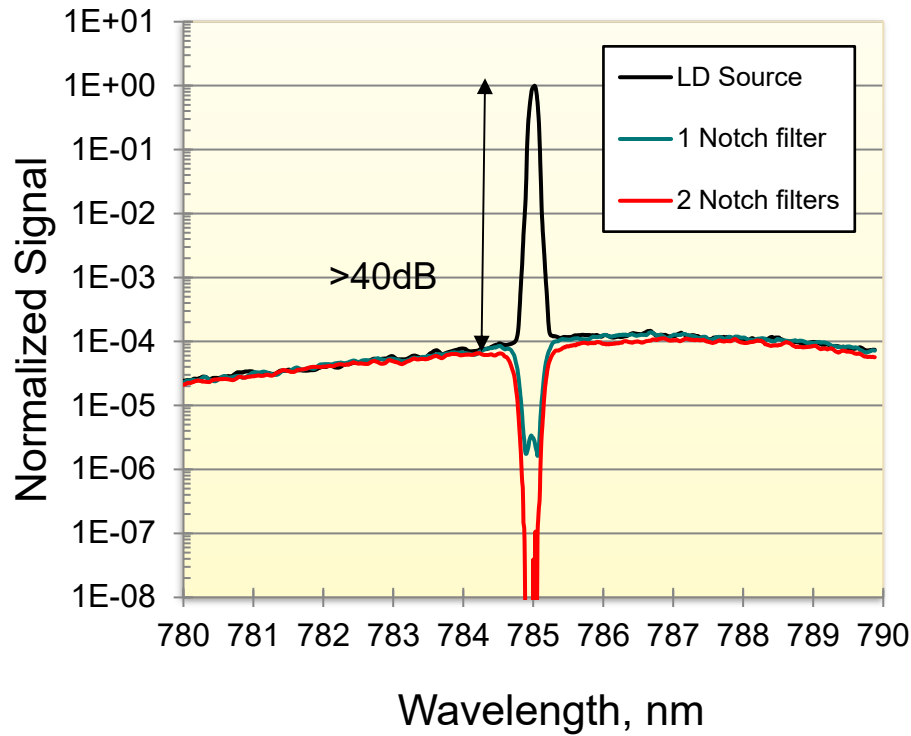


*Spectral profiles of the narrowest thin film filter available on the market and BragGrate Notch Filter (BNF). The bandwidth of a typical BNF is about 100-200 pm, whereas bandwidth of TF filters can't be narrower than 2-3 nm.*

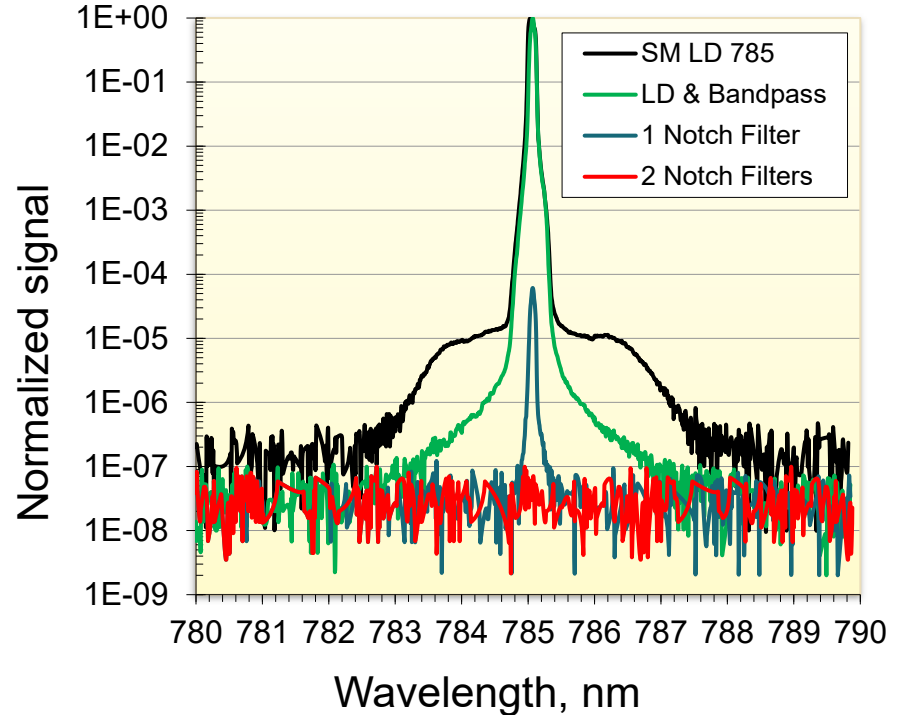
*Optical density of single BNF is limited to about OD4 and, thus, to provide sufficient Rayleigh light suppression depending on the measurement wavelength 2 to 3 filters have to be used in sequence*

*BNFs can be (optional) mounted in Ø1" round aluminum holders for easy use with standard opto-mechanical assemblies*

# Laser line “cleaning” and suppression



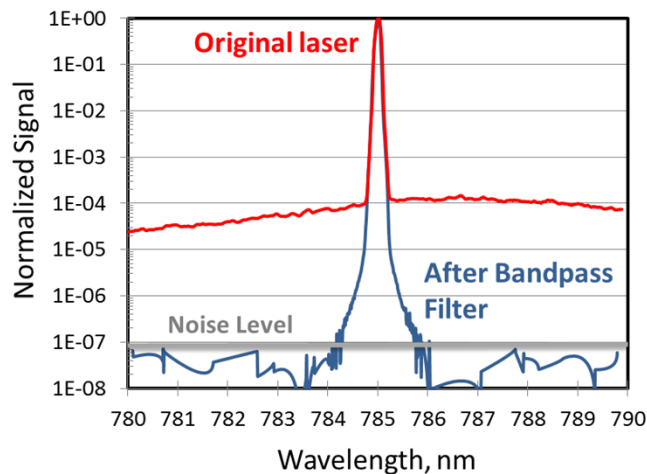
*Demonstration of 785 nm laser line suppression by 2 BNFs. ASE background was not removed for this demonstration. The line width of the notch filters is almost identical to the linewidth of the laser and, thus, the line is rejected completely without removing the background. That is in the case of Raman measurements the line is removed without affecting ultra low frequency modes down to  $5 \text{ cm}^{-1}$ .*



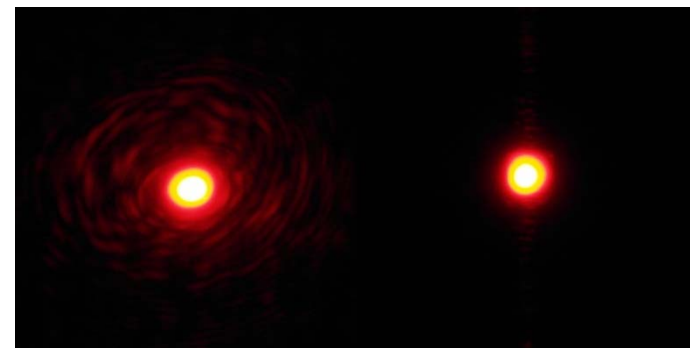
*Demonstration of 785 nm laser line cleaning by BPF and suppression by 2 BNFs. The original (black-line) spectrum was cleaned with a thin-film bandpass filter. Typical “shoulders” are seen which correspond to the linewidth of a thin film bandpass. After cleaning the laser with BPF the “shoulders” are removed. The figure shows that the cleaned laser line can be fully suppressed by sequential positioning of 2 BNFs*

# BragGrate™ Bandpass Filter (laser line cleaning)

- ❖ To achieve ULF Raman measurements, the laser spectral noise has to be removed as close as possible to the laser line. Standard Bandpass filters have the line width of 200-300  $\text{cm}^{-1}$  and, thus, all spectral noise below 200  $\text{cm}^{-1}$  would be visible in ULF Raman spectra interfering with measured Raman bands
- ❖ BragGrate™ Bandpass Filter (BPF) has the linewidth  $\sim 5 \text{ cm}^{-1}$  (FWHM) and, thus, removes laser noise down to 5  $\text{cm}^{-1}$  with suppression up to -70 dB
- ❖ BPF is a reflecting VBG which diffraction efficiency and other parameters are optimized for best noise removal close to the laser line
- ❖ Wavelength Range 400 nm to 2  $\mu\text{m}$  (standard wavelengths: 405, 488, 514, 532, 633, 785, 1064 nm)
- ❖ Standard BPF dimensions:  $5 \times 5 \times 2 \text{ mm}^3$  (785 nm filters are typically different in size)
- ❖ BPFs can be mounted in 1" or 0.5" mm round aluminum holders to be used with standard opto-mechanical mounts
- ❖ BPFs provide both spectral and spatial filtering as shown in figures below

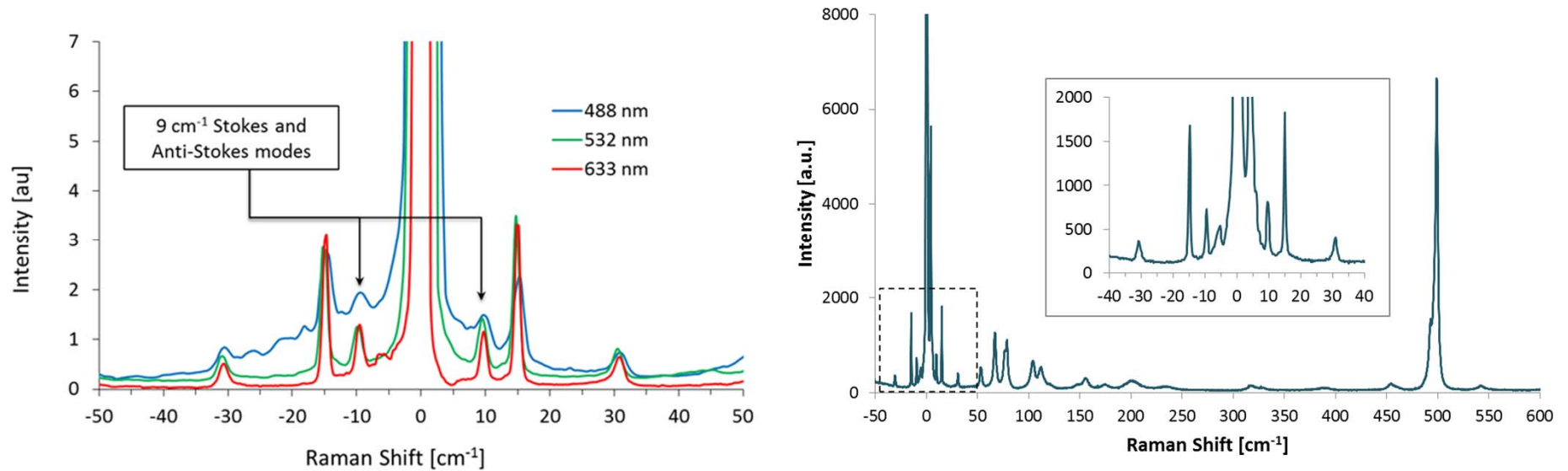


Spectral filtering of laser light with BPF. Red line: spectrum of a 785 nm diode laser with ASE background. Blue line: BPF removes the ASE background in immediate vicinity of the laser line. LD light beam cleaned with BPF enabled ULF Raman measurement down to 5  $\text{cm}^{-1}$



Spatial filtering of laser light with BPF. Left panel: far field image of HeNe laser beam profile without cleaning. Right panel: HeNe laser beam profile after spatial filtering with BPF. At the same time the laser is spectrally cleaned to -70 dB as close as 5  $\text{cm}^{-1}$  from the laser line

# Examples: ULF Raman measurements of L-Cystine

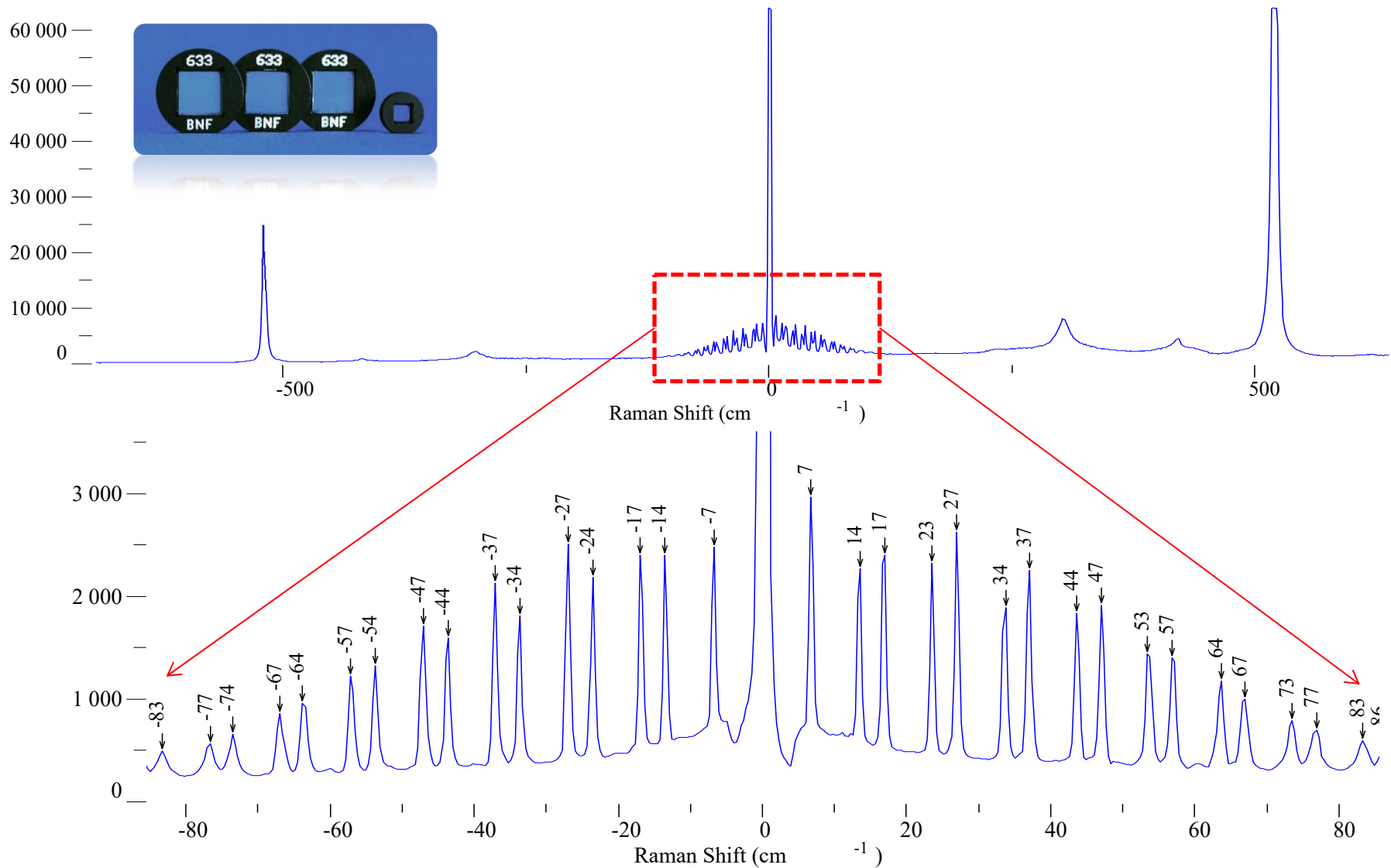


Ultra-low frequency measurements of L-Cystine at 4 different wavelengths: 488, 532, 633 nm (left) and 785 nm (right)



*data courtesy of Horiba Jobin Yvon*

# Examples: ULF Raman spectrum of SiGe superlattice

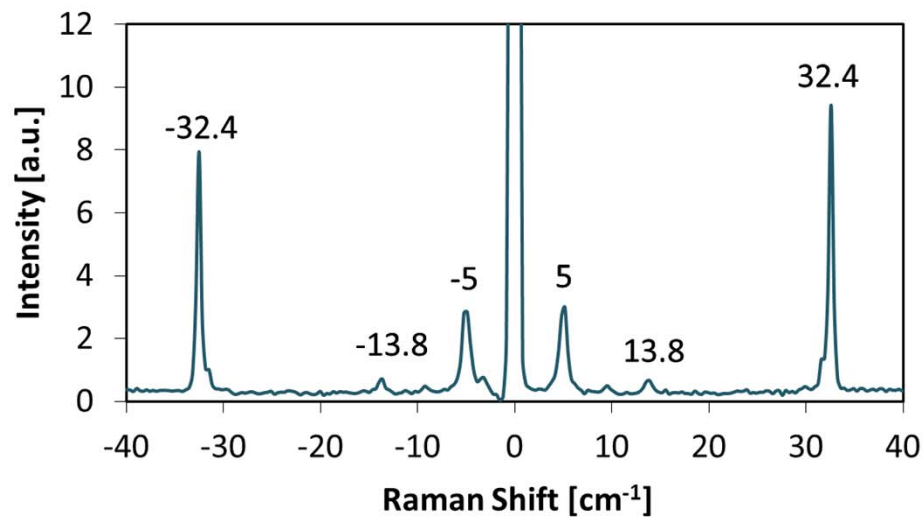


data courtesy of :

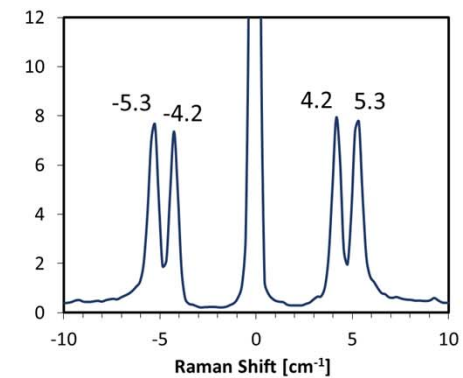
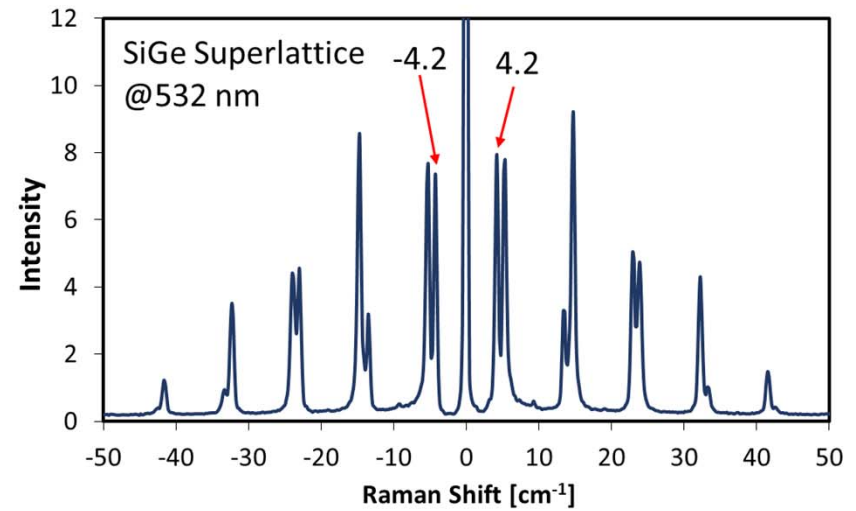
P. H. Tan, State Key Laboratory for SL and Microstr., Institute of Semiconductors, Beijing, P. R. China; K. Brunner, University Wuerzburg, Germany

# Examples: ULF Raman spectra at 5 cm<sup>-1</sup> and below

ULF Raman spectrum of several layers of MoS<sub>2</sub> flakes



Data courtesy of P. H. Tan, State Key Laboratory for SL and Microstr.,  
Institute of Semiconductors, Beijing, P. R. China;



Data courtesy of HORIBA; measured with LabRAM HR Evolution

# BragGrate™ Raman filters in work: selected publications

- ◆ Glebov et al., "Volume Bragg gratings as ultra-narrow and multiband optical filters", Proc. SPIE Vol. 8428, 84280C (2012), invited paper
- ◆ Tan et al., "The shear mode of multilayer graphene," **Nature**, Materials 11, 294–300 (2012).
- ◆ Ferrari et al., "Raman Spectroscopy as a versatile tool for studying the properties of graphene," **Nature**, Nanotechnology 8, 236-246 (2013)
- ◆ Chen et al., "Electronic Raman Scattering On Individual Semiconducting Single Walled Carbon Nanotubes," **Nature**, Scientific Reports 4, No. 5969 (2014)
- ◆ Nims et al., "Low frequency Raman Spectroscopy for micron-scale and in vivo characterization of elemental sulfur in microbial samples" **Nature**, Scientific Reports 9, No. 7971 (2019)
- ◆ Horiue et al., "Raman spectroscopic signatures of carotenoids and polyenes enable label-free visualization of microbial distributions within pink biofilms" **Nature**, Scientific Reports 10, No. 7704 (2020)
- ◆ Rahaman et al., "Fano resonance of Li-doped KTa<sub>1-x</sub>Nb<sub>x</sub>O<sub>3</sub> single crystals studied by Raman scattering" **Nature**, Scientific Reports 6, No. 23898 (2016)
- ◆ Helal et al., "Role of polar nanoregions with weak random fields in Pb-based perovskite ferroelectrics" **Nature**, Scientific Reports 7, No. 44448 (2017)
- ◆ Ge et al., "Coherent Longitudinal Acoustic Phonon Approaching THz Frequency in Multilayer MoS<sub>2</sub>," **Nature**, Scientific Reports 4, No. 5722 (2014)
- ◆ Cong et al., "Enhanced ultra-low-frequency interlayer shear modes in folded graphene layers," **Nature**, Communications 5, No. 4709 (2014)
- ◆ Wu et al., "Resonant Raman spectroscopy of twisted multilayer graphene," **Nature**, Communications 5, No. 5309 (2014)
- ◆ Huang et al., "Tuning inelastic light scattering via symmetry control in the two-dimensional magnet CrI<sub>3</sub>" **Nature**, Nanotechnology 15, 212–216 (2020)
- ◆ Zhu et al., "Tuning thermal conductivity in molybdenum disulfide by electrochemical intercalation" **Nature**, Communications 7, No. 13211 (2016)
- ◆ Zhang et al., Raman signatures of inversion symmetry breaking and structural phase transition in type-II Weyl semimetal MoTe<sub>2</sub>" **Nature**, Communications 7, No. 13552 (2016)
- ◆ Lin et al., "Cross-dimensional electron-phonon coupling in van der Waals heterostructures" **Nature**, Communications 10, No. 2419 (2019)
- ◆ Richard-Lacroix & Volker Deckert, "Direct molecular-level near-field plasmon and temperature assessment in a single plasmonic hotspot" **Nature**, Light: Science & Applications 9, No. 35 (2020)
- ◆ Iacobucci et al., "Three-dimensional microporous graphene decorated with lithium" **IOP Science**, Nanotechnology 29, 405707 (2018)
- ◆ Bang et al., "Compact noise-filtering volume gratings for holographic displays" **Optics Letters** 44, Issue 9, 2133-2136 (2019)
- ◆ Liu et al., "Filter-based ultralow-frequency Raman measurement down to 2 cm<sup>-1</sup> for fast Brillouin spectroscopy measurement" **Review of Scientific Instruments** 88, 053110 (2017)
- ◆ Bouyrie et al., "From crystal to glass-like thermal conductivity in crystalline minerals" **Phys. Chem. Chem. Phys.**, 17, 19751-19758 (2015)
- ◆ Ripanti et al., "Polarization Effects of Transversal and Longitudinal Optical Phonons in Bundles of Multiwall Carbon Nanotubes" **J. Phys. Chem. C** 123, 32, 20013–20019 (2019)
- ◆ Hehlen et al., "Soft-mode dynamics in micrograin and nanograin ceramics of strontium titanate observed by hyper-Raman scattering", **Phys. Rev. B** 87, 014303 (2013)
- ◆ Saviot et al., "Quasi-free nanoparticle vibrations in a highly-compressed ZrO<sub>2</sub> nanopowder", **J. Phys. Chem. C** 116, 22043 (2012)
- ◆ Vincent et al., "A compact new incoherent Thomson scattering diagnostic for low-temperature plasma studies" **IOP Science**, Plasma Sources Sci. Technol. 27 055002 (2018)
- ◆ Klarenaar et al., "How dielectric, metallic and liquid targets influence the evolution of electron properties in a pulsed He jet measured by Thomson and Raman scattering" **IOP Science**, Plasma Sources Sci. Technol. 27 085004 (2018)